KSME

Springer

Journal of Mechanical Science and Technology 34 (12) 2020

Original Article
DOI 10.1007/s12206-020-1124-1

Keywords:
· Self-tuning rule
· Sliding mode control
· Position control
· DC motor
· Recursive least squares
· Forgetting factor
· Power consumption

Correspondence to:
Jaho Seo
Jaho.Seo@uoit.ca

Citation:
Oh, K., Seo, J. (2020). Recursive least squares based sliding mode approach for position control of DC motors with self-tuning rule. Journal of Mechanical Science and Technology 34 (12) (2020) 5223~5237.
http://doi.org/10.1007/s12206-020-1124-1

Received January 10th, 2020
Revised August 3rd, 2020
Accepted September 14th, 2020

† Recommended by Editor
Ja Choon Koo

Recursive least squares based sliding mode approach for position control of DC motors with self-tuning rule

Kwangseok Oh[1] and Jaho Seo[2]

[1]School of ICT, Robotics & Mechanical Engineering, Hankyong National University, 327, Jungang-ro, Anseong-si, Gyeonggi-do, Korea, [2]Department of Automotive and Mechatronics Engineering, Ontario Tech University, 2000 Simcoe Street North, Oshawa, ON L1G 0C5, Canada

Abstract In this paper, a self-tuning rule-based position control algorithm is proposed for DC motors with system parameter estimation using the recursive least squares method. First, a mathematical model of the angular position control of a DC motor was derived. Next, the time-varying parameters including the rotational inertia in the model were estimated using the RLS method along with multiple forgetting factors without prior knowledge of the system. Based on the derived model and the parameter estimation, a sliding mode control algorithm was designed by applying a self-tuning rule that enables the magnitude of the voltage input to be adaptively adjusted for improvement of the energy efficiency. The performance of the designed control algorithm was then experimentally evaluated under several different load conditions. Finally, the evaluation results show that the designed controller achieves a satisfactory capability for a DC motor to deal with both tracking accuracy and energy efficiency without prior knowledge of the system.

1. Introduction

As a class of robust control, a sliding mode control technique enables the computation of control inputs to minimize errors despite the existence of bounded disturbances. In addition, various robust control algorithms have been developed, including H-infinity control, quantitative feedback theory, and linear quadratic Gaussian control. These robust control algorithms generally require relatively high computing power or exact knowledge of the systems to compute the control input and achieve a reasonably secure control performance. However, it is not easy to acquire the exact knowledge of a system if the characteristics of the system and the environmental conditions change dynamically in the real world. This change can have an extremely negative effect on control performance. To address the issue of control when the knowledge of a system is insufficient, various estimation algorithms have been developed in the area of sensorless and robust control for DC motors.

Liem et al. [1] presented a novel method for estimating the load torque of a DC motor shaft using a modeling method based on an online tuning grey fuzzy proportional integral derivative (PID) controller. Jesus et al. [2] developed an algebraic algorithm for online load estimation based on a boost-converter-driven DC motor system. In addition, by addressing cost and reliability problems, Shah et al. [3] designed a speed observer following an immersion and invariance technique that can be used for machine rotation. Algorithms proposed in previous studies [1-3] were designed based on the given system parameters. However, there is a limitation to such studies because the performance of the algorithms can be degraded if the parameters are incorrect or there are parameter uncertainties from changes in the environmental conditions.

Numerous studies related to adaptive and robust control for overcoming such limitations have been conducted. In the early development of adaptive and robust control algorithms, most of the algorithms were based on adaptive control laws such as gradient and Lyapunov methods.

The former control algorithms such as a model reference adaptive control algorithm require a reference model and an adaptive control law from the Lyapunov or gradient methods. Meanwhile, control algorithms have been developed using techniques such as an observer and artificial intelligence for robust control despite the existence of internal and external disturbances.

Shi et al. [4] presented a torque control algorithm to reduce the torque ripples of a brushless DC motor using two switching tables with the main and subsidiary vectors. Rubaai and Young [5] developed a control method for brushless DC motor drives using different fuzzy neural network learning, and they examined their algorithm using a simple pattern matching application. Hu et al. [6] presented an adaptive robust triple-step control algorithm for compensating the cogging torque and model uncertainty based on the estimation algorithm applied. In addition, Dao and Lee [7] developed a control algorithm for a five-level hybrid flying-capacitor inverter, the structure of which stems from a conventional five-level active neutral-point-clamped topology, and was realized by dividing the DC-link stage into three series-connected capacitors. You et al. [8] developed a robust position tracking control algorithm for a DC motor with external disturbance and system uncertainties based on the extended state observer. The extended state observer was designed to estimate the disturbance and full states. Rodríguez-Molina et al. [9] presented a comparative study on different meta-heuristic techniques with adaptive control for speed regulation of a DC motor with parameter uncertainties. The adaptive control algorithm was established for a constrained dynamic optimization problem. Kofinas and Dounis [10] proposed an online tuning algorithm for the PID parameters used to control the speed of a DC motor based on a hybrid Zeigler-Nichols reinforcement-learning approach. After a careful review of previous studies on DC motor control using various estimation and control methods, it is found that most studies have been conducted based on knowledge of the system. In other words, the estimation and control algorithms are based on the actual or nominal system parameters. To secure the control performance despite internal and external disturbances, some stochastic and real-time learning algorithms have been developed. In addition, rule-based control and learning algorithms have been integrated to improve the control performance of DC motors.

Premkumar and Manikandan [11, 12] presented a proportional derivative integral control algorithm for the speed control of a brushless direct current drive based on the fuzzy theory. In previous studies [13, 14], all parameters used were based on fuzzy logic, and an adaptive algorithm was designed to cope with the parameter uncertainties. The scaling factor for the inputs and outputs of the developed fuzzy logic controller influences the performance of the control system. In addition, the scaling factor of a fractional-order fuzzy PID controller tuned using a cuckoo search algorithm was presented by Sharma et al. [15]. Moreover, Thomas [16] proposed a linear quadratic controller based on a modified cultural artificial fish swarm algorithm. Based on the control algorithm, the optimal value was computed for an improved output torque of the motor.

Hsu and Lee [17] proposed an adaptive PID controller, which is composed of a PID controller and a fuzzy compensator. The controller was designed such that the control gains are tuned automatically based on the gradient descent method and a fuzzy compensator to eliminate the effect of approximation errors. As indicated in studies related to a fuzzy-logic based controller, the performance of the system depends on both the scaling factors and positions of the membership functions for the inputs and outputs of the controller.

Mondal and Mahanta [18] proposed an adaptive second-order terminal sliding mode control algorithm for controlling robotic manipulators. Utkin and Poznyak [19] developed an adaptation methodology to search the minimum possible control value through evaluations of the equivalent control using a low-pass filter. Mollaee and Tirandaz [20] presented a load torque estimation algorithm of an induction motor (IM) with uncertainty using a dynamic sliding mode controller based on Lyapunov theory. These studies focused on resolving two representative problems of the sliding mode control, which are chattering and high activity of control action. In the studies, online tuning rules of the magnitude injection term for adaptive sliding mode control based on stability conditions were developed. However, this approach has a limitation in that accurate identification of types and magnitude of disturbance is difficult to achieve. Specifically, if the disturbance is changed abruptly, the magnitude of an injection term may not be tuned reasonably. This may lead to degrade the control performance and lose the stability of a control system. To overcome this problem, the disturbance was estimated directly using recursive least squares (RLS) with a forgetting factor in this study where a bounded value of the disturbance is not constant and can be varied with the estimated disturbance to secure control stability. In our proposed method, the disturbance estimated by RLS includes system parameters and thus the designed controller does not require a system parameter. The objective of the present study is the design of a sliding mode controller for the position control of a DC motor with a self-tuning rule using the RLS method. The main contributions of this study can be summarized as follows.

1) The controller proposed in this study can compute the control input (voltage input) for a DC motor to track the desired angular position robustly without the use of any system parameters.

2) Using the self-tuning rule designed in this study, the magnitude of a control input can be minimized to improve energy efficiency without any loss of control stability.

With the self-turning rule, RLS with multiple forgetting factors was applied for parameter estimation. A mathematical model of an actual DC motor system was derived for the parameter estimation. Based on the parameters estimated using RLS, a sliding mode controller was designed to compute an input for the position control of the DC motor. In addition, the self-tuning

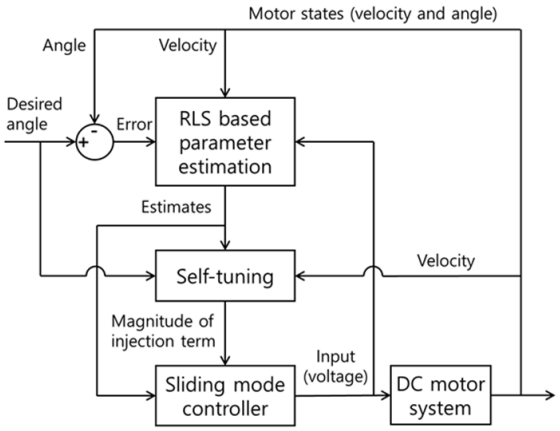

Fig. 1. Flow chart for the correction of the roll forming process design.

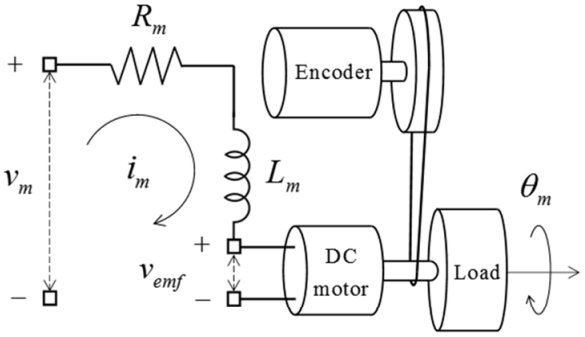

Fig. 2. Electric circuit diagram of the DC motor system.

rule was designed to tune the magnitude of the control input (voltage input) for the DC motor. An actual test platform of a DC motor was used for performance evaluation with various desired inputs such as ramp and sinusoidal inputs. The actual test platform was equipped with a rotary type encoder that can obtain the pulse signals for rotational motion. The performance evaluation was conducted under various load conditions using a detachable attachment for the load. The design of the controllers and their performance evaluations were carried out using a MATLAB/Simulink environment. The performance of the designed controllers was compared to that of other types of controllers such as a PID controller, linear quadratic regulator (LQR), and sliding mode control (SMC) without a self-tuning rule.

The rest of this paper is organized as follows. Sec. 2 describes the concept of the proposed control algorithm. Sec. 3 describes the self-tuning rule-based sliding mode controller. The evaluation results of the control performance are provided in Sec. 4. Finally, in Sec. 5, some concluding remarks are provided along with areas of future study.

2. Concept of control algorithm

Fig. 1 shows an overall model schematic demonstrating the concept of the proposed position control algorithm for a DC motor.

In the RLS-based parameter estimation block shown in the figure, the system parameters of the DC motor used for adaptive control are estimated using the RLS with multiple forgetting factors. The estimated parameters of the DC motor are used as inputs to the self-tuning and sliding mode controller blocks. In the self-tuning block, the self-tuning rules were designed to compute the magnitude of the injection term in real-time based on the computed disturbance using the estimated parameters, motor states, and desired angles. The DC motor system block represents an actual test platform of the DC motor used for the performance evaluation. The input of this block is the voltage command and the outputs are the angle and velocity as measured using a rotary type encoder. The next section describes the self-tuning rule-based sliding mode control algorithm.

3. Self-tuning rule-based sliding mode control

In this study, a sliding mode control algorithm with self-tuning rules was adopted for position control of the DC motor. Error dynamics were derived based on the actual DC motor system equipped with a rotary encoder to measure the angular position. The parameters of the derived error dynamics were estimated using the RLS with multiple forgetting factors. The sliding mode control algorithm was constructed for position control with a self-tuning rule. The self-tuning rules were designed to adjust the magnitude of the input computed by the sliding mode control algorithm through a parameter estimation.

3.1 Parameter estimation of system dynamics

To derive the system dynamic equations of the considered DC motor, its mathematical model, shown in Fig. 2, was constructed.

In the figure, v_m, i_m, and v_{emf} represent the input voltage, current, and back electromotive force voltage, respectively. θ_m is the angular position of the DC motor, R_m and L_m and represent the resistance and inductance in the circuit. The DC motor system described in Fig. 2 is the actual system used for the experiments conducted in this study. The mathematical model of the DC motor system with respect to the angular velocity can be derived using two equations such as electrical and mechanical equations. The equations are based on the Kirchhoff's voltage and Newton's second law as follows:

$$v_m(t) - R_m i_m(t) - L_m \frac{di_m(t)}{dt} - k_m \omega_m(t) = 0 \quad (1)$$

$$J_{eq}(t)\dot{\omega}_m(t) = \tau_m(t) = k_t i_m(t)\,. \quad (2)$$

Under the assumption that the inductance is sufficiently smaller than the resistance, the resulting dynamic Eq. (3) of the DC motor can be obtained by inputting the current from Eq. (1) into Eq. (2).

$$\dot{\omega}_m(t) + A(t)\omega_m(t) = B(t)v_m(t) \tag{3}$$

$$A(t) = \frac{k_t k_m}{J_{eq}(t)R_m},\ B(t) = \frac{k_t}{J_{eq}(t)R_m}. \tag{4}$$

The equivalent rotational inertia is a time-varying parameter because the load can be varied based on the environmental conditions or tasks. Therefore, Eq. (3) is a linear time-variant system, and the resulting parameters such as $A(t)$ and $B(t)$ were estimated for adaptive angular position control. For parameter estimation, the discrete RLS method was used with multiple forgetting factors [21]. The output (y), regressor (ϕ), and estimate (θ) were defined for the parameter estimation as follows.

$$y = \phi^T\theta,\ \phi = [\phi_1 \quad \phi_2]^T,\ \theta = [\theta_1 \quad \theta_2]^T \tag{5}$$

where ϕ , y , θ represent the regressor, output, and estimate, respectively. They are defined for the discrete RLS through the discretization of Eq. (3) as follows:

$$\phi = [\phi_1 \quad \phi_2]^T = [-\omega_m(k-1)\Delta t \quad v_m(k-1)]^T \tag{6}$$

$$\theta = [\theta_1 \quad \theta_2]^T = [A(k) \quad B(k)]^T \tag{7}$$

$$y = \omega_m(k) - \omega_m(k-1). \tag{8}$$

If the values of parameters $A(t)$ and $B(t)$ of a system change abruptly, a periodic resetting method may be proper for capturing the new values of the system parameters. However, if the system parameters vary continuously and slowly, an estimation scheme with forgetting is effective. The system parameters $A(t)$ and $B(t)$ vary with a change in the equivalent rotational inertia and some values of the coefficients. The forgetting used in the least square method gives less weight to older data and more weight to recent data. In this study, two forgetting factors λ_1 and λ_2 were applied to the RLS method and the loss-function was defined using multiple forgetting factors as follows:

$$\begin{aligned} &J\left(\hat{\theta}_1(k), \hat{\theta}_2(k), k\right) \\ &= \frac{1}{2}\sum_{i=1}^{k}\lambda_1^{k-i}\left(y(i) - \phi_1(i)\hat{\theta}_1(k) - \phi_2(i)\theta_2(k)\right)^2 + \\ &\quad \frac{1}{2}\sum_{i=1}^{k}\lambda_2^{k-i}\left(y(i) - \phi_1(i)\theta_1(k) - \phi_2(i)\hat{\theta}_2(k)\right)^2. \end{aligned} \tag{9}$$

The degrees of freedom can be further provided for tuning the estimator using multiple forgetting factors. As a result, varying parameters with different rates can be tracked more precisely. The optimal estimates minimizing the loss function are obtained through a differentiation of the loss function with respect to each estimate.

$$\hat{\theta}_1(k) = \left(\sum_{i=1}^{k}\lambda_1^{k-i}\phi_1(i)^2\right)^{-1} \times \left(\sum_{i=1}^{k}\lambda_1^{k-i}\left(y(i) - \phi_2(i)\theta_2(k)\right)\right) \tag{10}$$

$$\hat{\theta}_2(k) = \left(\sum_{i=1}^{k}\lambda_2^{k-i}\phi_2(i)^2\right)^{-1} \times \left(\sum_{i=1}^{k}\lambda_2^{k-i}\left(y(i) - \phi_1(i)\theta_1(k)\right)\right). \tag{11}$$

Based on Eqs. (10) and (11) above, a recursive form is required for a real-time estimation, and can be deduced as follows:

$$\begin{aligned} \hat{\theta}_1(k) &= \hat{\theta}_1(k-1) + \\ &\quad L_1(k)\left(y(k) - \phi_1(k)\hat{\theta}_1(k-1) - \phi_2(k)\theta_2(k)\right) \end{aligned} \tag{12}$$

$$\begin{aligned} \hat{\theta}_2(k) &= \hat{\theta}_2(k-1) + \\ &\quad L_2(k)\left(y(k) - \phi_1(k)\theta_1(k) - \phi_2(k)\hat{\theta}_2(k-1)\right) \end{aligned} \tag{13}$$

where

$$\begin{aligned} L_1(k) &= P_1(k-1)\phi_1(k)\left(\lambda_1 + \phi_1^T(k)P_1(k-1)\phi_1(k)\right)^{-1} \\ P_1(k) &= \left(I - L_1(k)\phi_1^T(k)\right)P_1(k-1)/\lambda_1 \\ L_2(k) &= P_2(k-1)\phi_2(k)\left(\lambda_2 + \phi_2^T(k)P_2(k-1)\phi_2(k)\right)^{-1} \\ P_2(k) &= \left(I - L_2(k)\phi_2^T(k)\right)P_2(k-1)/\lambda_2. \end{aligned}$$

Under the assumption that the actual and estimated values are very close to each other or within the algorithm region of convergence, Eqs. (12) and (13) can be rewritten in matrix form as follows:

$$\begin{aligned} \begin{bmatrix}\hat{\theta}_1(k)\\ \hat{\theta}_2(k)\end{bmatrix} &= \begin{bmatrix}1 & L_1(k)\phi_2(k)\\ L_2(k)\phi_1(k) & 1\end{bmatrix}^{-1} \times \\ &\quad \begin{bmatrix}\hat{\theta}_1(k-1) + L_1(k)\left(y(k) - \phi_1(k)\hat{\theta}_1(k-1)\right)\\ \hat{\theta}_2(k-1) + L_2(k)\left(y(k) - \phi_2(k)\hat{\theta}_2(k-1)\right)\end{bmatrix}. \end{aligned} \tag{14}$$

The determinant of the following matrix is non-zero because P_1 and P_2 are always positive.

$$\begin{bmatrix}1 & L_1(k)\phi_2(k)\\ L_2(k)\phi_1(k) & 1\end{bmatrix}. \tag{15}$$

Based on the RLS with multiple forgetting factors, the parameters $A(t)$ and $B(t)$ were estimated and used for the sliding mode control algorithm. The next sub-section describes this algorithm.

3.2 Sliding mode control algorithm

The sliding mode control algorithm was adopted to compute the adaptive and robust control input for position control of the DC motor. To design the sliding mode control algorithm, error states P_1 and P_2 are defined as follows:

$$e_1(t) = \theta_{m,des}(t) - \theta_m(t) \tag{16}$$

$$e_2(t) = \omega_{m,des}(t) - \omega_m(t) \tag{17}$$

where e_1 and e_2 represent the angle and velocity error states, respectively. θ_m and ω_m are the DC motor angle and velocity. Based on the defined error states in Eqs. (16) and (17), error dynamics can be derived using Eq. (3) as follows:

$$\dot{e}_1(t) = \dot{\theta}_{m,des}(t) - \dot{\theta}_m(t) = e_2(t) \tag{18}$$

$$\dot{e}_2(t) = \dot{\omega}_{m,des}(t) + A(t)\omega_m(t) - B(t)v_m(t) . \tag{19}$$

In addition, the error dynamics can be rewritten in a state-space form with a disturbance term.

$$\dot{e}_1(t) = e_2(t) \tag{20}$$

$$\dot{e}_2(t) = -B(t)v_m(t) + \underbrace{\dot{\omega}_{m,des}(t) + A(t)\omega_m(t)}_{Disturbance, f(\dot{\omega}_{m,des}, A, \omega_m)} . \tag{21}$$

The disturbance term in Eq. (21) consists of time-varying values such as the desired acceleration, parameter $A(t)$, and velocity. Under the assumption that there are physical constraints such as a variation in inertia and maximum velocity and acceleration of the DC motor, it can be reasonably defined that the disturbance is bounded but time-varying, i.e., $\left| f(\omega_{m,des}(t), A(t), \omega_m(t)) \right| \le L(t)$. The following sliding surface for the error states was defined as follows:

$$\sigma(e_1(t), e_2(t)) = e_2(t) + ce_1(t), \;\; c > 0 . \tag{22}$$

Using the sliding surface, the following Lyapunov function candidate was defined for a derivation of the control input and checking the stability of the control algorithm.

$$V = \frac{1}{2}\sigma^2 \tag{23}$$

where V and σ represent Lyapunov function and sliding surface, respectively. It was found that the following two conditions are satisfied and result in asymptotic stability near the equilibrium point $\sigma = 0$ and a finite time convergence [22, 23].

(A) $\dot{V} \le -\alpha V^{1/2}, \; \alpha > 0$

(B) $\lim_{|\sigma| \to \infty} V = \infty$.

Condition (A) will drive the variable σ to zero in finite time and keep it at zero thereafter. The following equation describes the finite time inequality from the condition (A). The equation was derived using the methodology for separating variables and integration equality with the assumption that the value of Lyapunov function is zero at the reaching time t_r.

$$t_r \le \frac{2V^{1/2}(0)}{\alpha} . \tag{24}$$

To keep the derivative of Lyapunov function candidate negative, the input term of Eq. (21) is defined by selecting the injection term, $v = -\rho sign(\sigma)$ as follows.

$$-Bv_m(t) = -ce_2 + v . \tag{25}$$

The derivative of the Lyapunov function in Eq. (23) is derived by using Eqs. (22) and (25), and the definition of the injection term v as follows.

$$\begin{aligned} \dot{V} &= \sigma\dot{\sigma} = \sigma\left(\dot{e}_2 + c\dot{e}_1\right) \\ &= \sigma\left(-Bv_m + f + ce_2\right) = \sigma\left(v + f\right) . \end{aligned} \tag{26}$$

With the assumption that the value of the disturbance function $f(\omega_{m,des}(t), A(t), \omega_m(t))$ is bounded by L, Eq. (26) and the condition (A) related to the Lyapunov function can be rewritten as follows.

$$\dot{V} = \sigma\left(-\rho sign(\sigma) + f\right) \le -|\sigma|\left(\rho - L\right) \tag{27}$$

$$\dot{V} \le -\frac{\alpha}{\sqrt{2}}|\sigma| . \tag{28}$$

Based on Eqs. (27) and (28), the magnitude of the injection term ρ is computed with the bounded value and α in the condition (A) as below.

$$\rho(t) = L(t) + \alpha / 2 . \tag{29}$$

From Eqs. (27) and (29), it is found that the derivative of the Lyapunov function candidate is always negative. It is therefore reasonably confirmed that the sigma (σ) dynamics defined in Eq. (22) is asymptotically stable near the equilibrium point $\sigma = 0$. Based on Eq. (25), with the estimated parameter $\hat{B}(t)$, the voltage input $v_m(t)$ can be written using the error state $e_2(t)$ as follows:

$$v_m(t) = \frac{c}{\hat{B}(t)}e_2(t) + \frac{\rho(t)}{\hat{B}(t)}sign(\sigma) . \tag{30}$$

The voltage input is computed using the estimated parameters $\hat{B}(t)$, which include unknown parameters such as time-varying rotational inertia, torque constant, and resistance. Therefore, a proper voltage input can be computed for a change in the rotational inertia and unknown parameters of the DC motor. Since the magnitude of the injection term in Eq. (29) is a time-varying value and can influence the magnitude of the voltage input, the self-tuning rule has been proposed in this study to compute the proper voltage input based on a disturbance estimation. In addition, the control algorithm is asymptotically stable with a control input computed based on Eq. (30). However, a physical constraint such as an input voltage limit is not considered in the current research step. The next subsection describes the self-tuning rule.

Table 1. Algorithm of self-tuning rule.

Line	Self-tuning algorithm
1	Computation of the magnitude of the injection term
2	$\rho(k) = (1+r)D(k) + \alpha/2$
3	Comparison between the computed and minimum magnitudes
4	If $\rho(k) < \rho_{\min}$
5	$\rho(k) = \rho_{\min}$
6	End

3.3 Self-tuning rule

In this study, a self-tuning rule was designed to adjust the magnitude of the injection term of the sliding mode control. The main idea of the self-tuning rule is to tune the boundary value $L(t)$ described in Eq. (21) that is varied with the desired velocity $\omega_{m,des}(t)$, current velocity $\omega_m(t)$, and the estimated parameters $\hat{A}(t)$. A proper magnitude of the injection term can be found by selecting the boundary value $L(t)$. The selected $L(t)$ is slightly larger than the estimated disturbance by the RLS for the asymptotically stable condition because there exists the estimation error between the actual disturbance and estimated one. To design the self-tuning algorithm with an asymptotically stable condition, the time-varying disturbance $D(t)$ can be rewritten with time instance *k* as follows:

$$D(k) = \dot{\omega}_{m,des}(k) + \hat{A}(k)\omega_m(k). \tag{31}$$

Table 1 shows the self-tuning algorithm used for an adjustment of the magnitude of the injection term in sliding mode control. The proper boundary value $L(t)$ can be computed in real-time based on the desired and estimated disturbance values. Using the proper boundary value, the magnitude of the injection term can be computed as follows:

$$\rho(k) = (1+r)|D(k)| + \alpha/2. \tag{32}$$

The magnitude of the injection term was computed with the increasing ratio *r* (that is positive and $r \in (0,1)$) and a reduction of ratio α in real-time. However, an algorithm that restricts the computed magnitude of the injection term was designed using the minimum magnitude of the injection term. The increasing ratio, reduction ratio, and minimum magnitude of the injection term are experimentally determined design parameters. The increasing ratio defined for the self-tuning rule was determined experimentally by considering the estimation error between actual disturbance and estimated one. The reduction ratio and minimum magnitude of the injection term in Table 1 were also determined experimentally by using trial and error method to search the values that can reduce the magnitude of the injection rapidly without losing the control stability. Based on the self-tuning rule designed in this study, the sliding mode controller can compute the minimum control input without a loss of control stability that would improve energy efficiency. The next section describes the performance evaluation results on an actual test platform.

Table 2. Parameters of actual test platform.

Parameter	Unit	Description	Value
R_m	Ω	Resistance	8.4
k_t	Nm / A	Torque constant	0.042
k_m	V / (rad / s)	Back-EMF constant	0.042

Fig. 3. Actual test platform and removable attachment [Quanser - servo 2].

4. Performance evaluation

The performance evaluation described herein was conducted using an actual test platform of a DC motor equipped with a rotary type encoder. The voltage input of the test platform was limited within ±5 V. The control algorithm proposed in this study was designed in a MATLAB/Simulink environment. The angular position of the platform can be controlled by the controller and its input and output data can be collected in MATLAB/Simulink. A detachable cylindrical attachment was used to change the rotational inertia of the DC motor in the test platform. Fig. 3 shows the actual test platform with the detachable attachment used for the performance evaluation.

Table 2 shows the parameters of resistance, torque constant, and back-EMF constant representing the features of the actual test platform.

Using the test platform, the proposed position control algorithm was evaluated using several desired inputs and load conditions. Fig. 4 shows a model schematic of the structure of the controllers used for the performance evaluation.

For a reasonable evaluation and analysis, ramp and sinusoidal inputs were used as reference inputs. Each evaluation scenario (see Table 5) is classified into two sub-cases depending on whether it has the attachment.

For a comparative study with other control approaches, the PID and LQR control algorithms were considered. The PID control algorithm does not need the system information but does need to adjust the control gains to obtain an acceptable control performance. The LQR is an optimal control algorithm

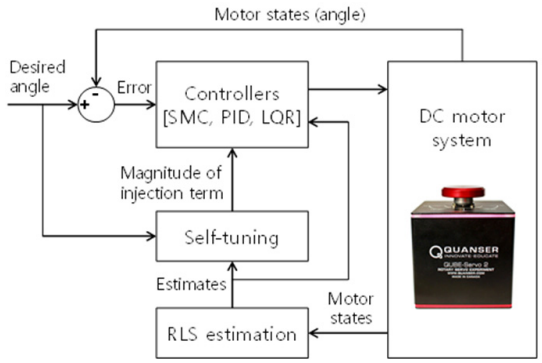

Fig. 4. Model schematics for performance evaluation.

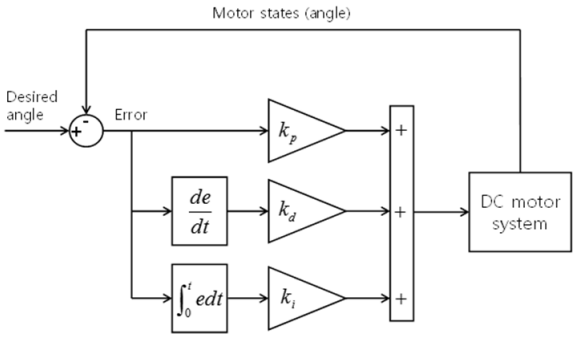

Fig. 5. Model schematics for PID control.

that requires an accurate mathematical model. The following sub-sections describe each control algorithm used for the performance evaluation.

4.1 PID control algorithm

Fig. 5 describes the model schematics for the PID controller-based algorithm.

The control law is as described below, and control gains such as proportional, integral, and derivative gains are as indicated in Table 3.

$$v_m(t) = k_p e_1(t) + k_d e_2(t) + k_i \int_0^t e_1(t)dt \tag{33}$$

where k_p, k_i, and k_d represent the proportional, integral, and derivative gains, respectively.

4.2 LQR control algorithm

Fig. 6 describes the model schematics for the LQR based control algorithm.

A linear quadratic regulator was used to derive the model-based control results. Based on the motor dynamics, a state-space equation for error dynamics was derived using the error state definition as follows.

Table 3. Simulation parameters for PID controller.

Parameter	Description	Value
k_p	Proportional gain	5.5
k_i	Integral gain	10
k_d	Derivative gain	0.25

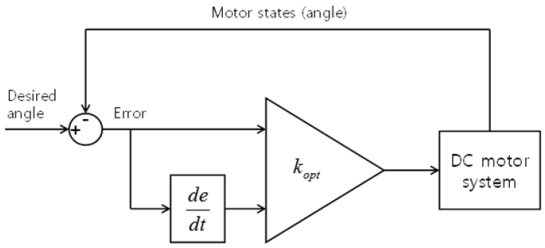

Fig. 6. Model schematics for LQR control.

$$e = \begin{bmatrix} e_1 & e_2 \end{bmatrix}^T = \begin{bmatrix} \theta_{m,des} - \theta_m & \dot{\theta}_{m,des} - \dot{\theta}_m \end{bmatrix}^T \tag{34}$$

$$\dot{e}(t) = A_e e(t) + B_e v_m(t) + w(t) \tag{35}$$

where

$$A_e = \begin{bmatrix} 0 & 1 \\ 0 & -A \end{bmatrix}, B_e = \begin{bmatrix} 0 \\ -B \end{bmatrix}, w = \begin{bmatrix} 0 \\ A\dot{\theta}_{m,des}(t) + \ddot{\theta}_{m,des}(t) \end{bmatrix}.$$

Here, A_e and B_e are computed using the actual values in Table 3, and A and B are constant parameters computed using the values in Table 2. To make the error dynamics asymptotically stable, the control law was defined as follows.

$$v_m(t) = -K_{opt} e(t) + r(t). \tag{36}$$

To reject the disturbance term $w(t)$, r is defined as follows:

$$r(t) = -A\dot{\theta}_{m,des}(t) - \ddot{\theta}_{m,des}(t). \tag{37}$$

The optimal control gain K_{opt} was computed, which minimizes the following performance index J.

$$J = \int_0^t \left(e^T Q e + v_m^T R v_m \right) dt. \tag{38}$$

The actual parameters used for the LQR controller are described in Table 4.

4.3 Evaluation results

The performance evaluation was conducted using two desired inputs such as ramp and sinusoidal inputs. Fig. 7 describes the desired inputs applied to the actual test platform.

Table 4. Simulation parameters for LQR controller.

Parameter	Description	Value
A	Motor parameter *A*	3.67
B	Motor parameter *B*	87.42
Q	Weighting matrix for state	$\begin{bmatrix} 20 & 0 \\ 0 & 1 \end{bmatrix}$
R	Weighting matrix for input	1
K_{opt}	Optimal control gain	$[-4.47 \quad -1.01]$

Table 5. Evaluation cases.

Cases	Load conditions	Desired inputs	Controllers
Case 1-1	w/o attachment	Ramp input	- SMC (w/o updating rule, fixed) - SMC (w/ updating rule) - PID - LQR
Case 1-2	w/ attachment		
Case 2-1	w/o attachment	Sinusoidal input	- SMC (w/o updating rule, fixed) - SMC (w/ updating rule) - PID - LQR
Case 2-2	w/ attachment		

Table 6. Simulation parameters used for performance evaluation.

Parameter	Unit	Description	Value
α	-	Reduction ratio	10
$\rho_{\min}$	-	Minimum magnitude of the injection term	5
c	-	Slope of the sliding surface	7

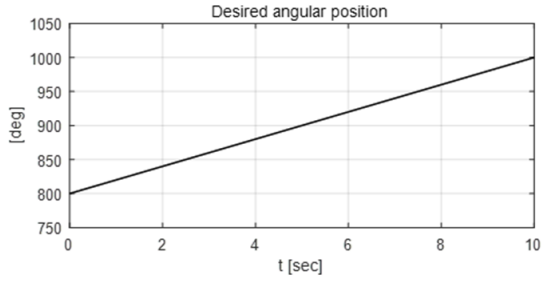

(a) Ramp input [20 deg/s]

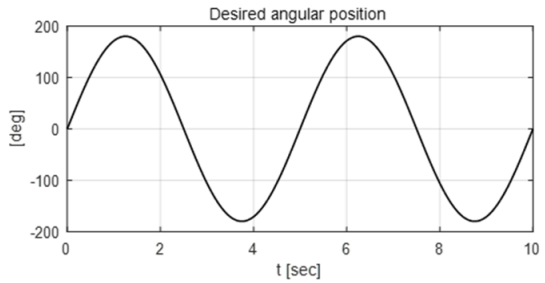

(b) Sinusoidal input [0.2 Hz, max 180 deg]

Fig. 7. Desired inputs for performance evaluation.

A total of four controllers were used to conduct the performance evaluation, which include the sliding mode controller (SMC) with a fixed ρ, SMC with an adaptive ρ, linear quadratic regulator (LQR), and PID controller. Table 5 shows the overall evaluation cases applied for the performance evaluation.

Table 6 shows the parameters used for the sliding mode control algorithm, self-tuning rule, and performance evaluation.

To compute the power consumption of the DC motor, the following power equation was used with the actual parameters shown in Table 2 based on Eq. (1).

$$P_m(t) = v_m(t) i_m(t) = v_m(t) \left(\frac{v_m(t) - k_m \omega_m(t)}{R_m} \right). \tag{39}$$

Using Eq. (39) above, the total power consumption *E* was computed through an integration of the power with respect to time as follows.

$$E(t) = \int_0^t v_m(t) \left(\frac{v_m(t) - k_m \omega_m(t)}{R_m} \right) dt. \tag{40}$$

Figs. 8-35 show the performance evaluation results conducted under various loads and desired input conditions.

Case 1-1: ramp input without attachment

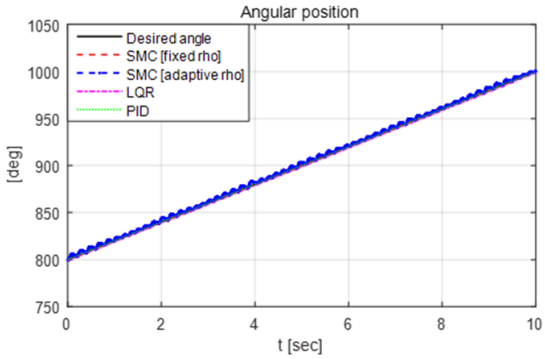

(a) Angles

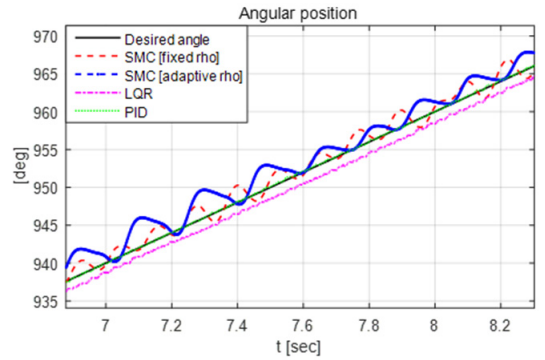

(b) Angles (zoom in)

Fig. 8. Desired and angular positions: case 1-1.

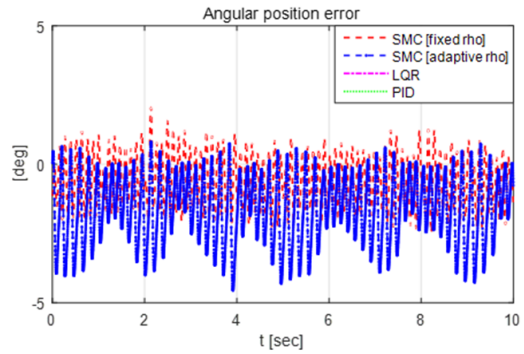

Fig. 9. Angular position errors: case 1-1.

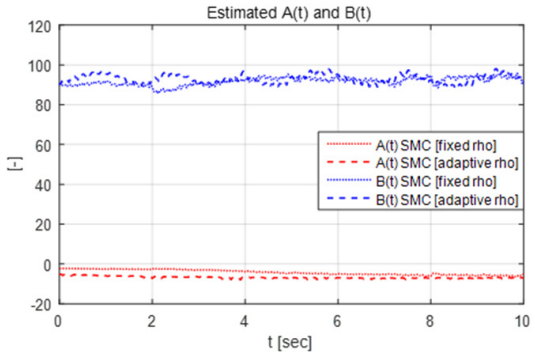

Fig. 10. Estimated parameters: case 1-1.

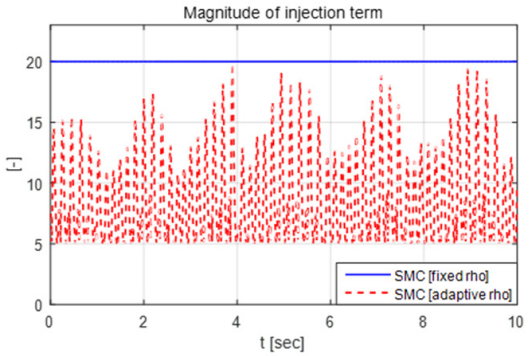

Fig. 11. Magnitude of injection term: case 1-1.

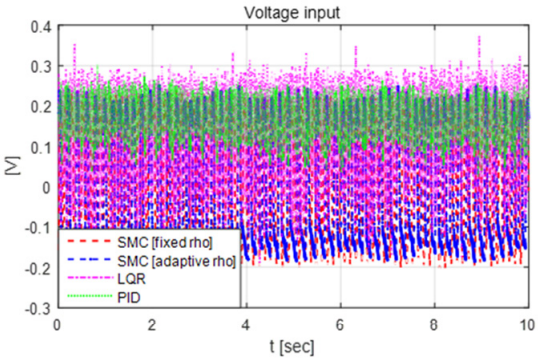

Fig. 12. Input voltage: case 1-1.

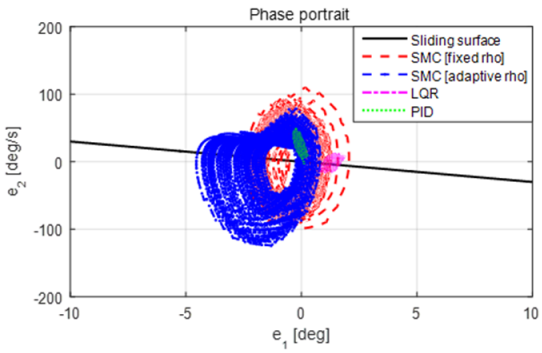

Fig. 13. Phase portrait: case 1-1.

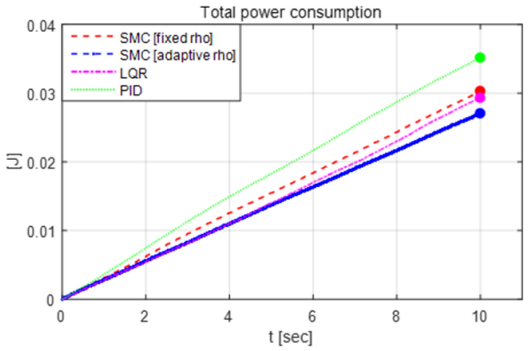

Fig. 14. Total power consumption: case 1-1.

Case 1-2: ramp input with attachment

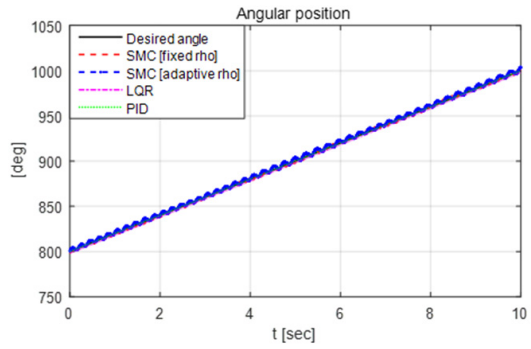

(a) Angles

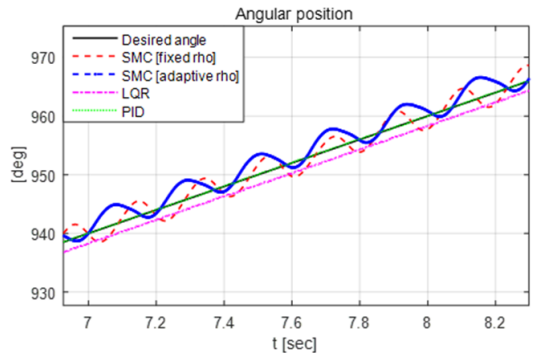

(b) Angles (zoom in)

Fig. 15. Desired and angular positions: case 1-2.

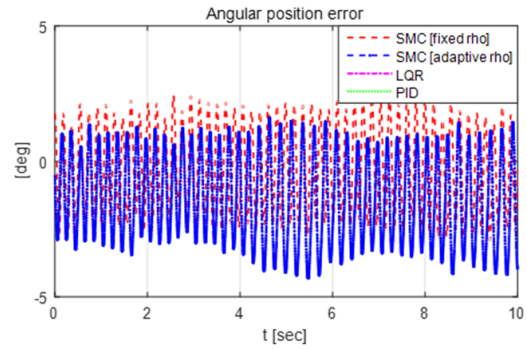

Fig. 16. Angular position errors: case 1-2.

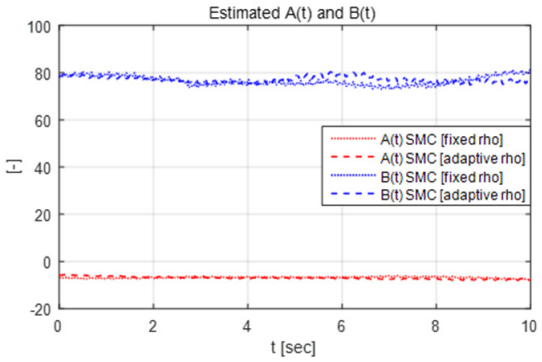

Fig. 17. Estimated parameters: case 1-2.

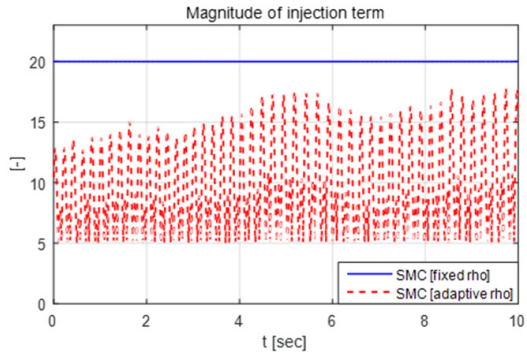

Fig. 18. Magnitude of injection term: case 1-2.

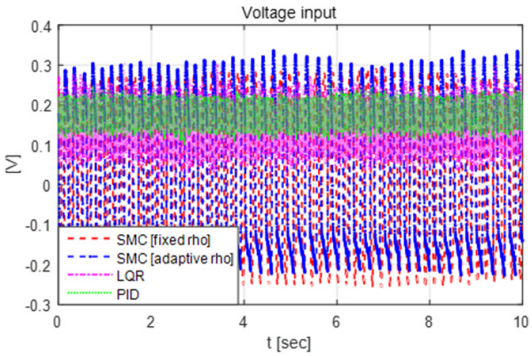

Fig. 19. Input voltage: case 1-2.

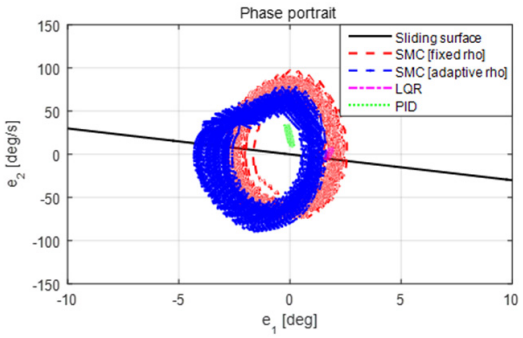

Fig. 20. Phase portrait: case 1-2.

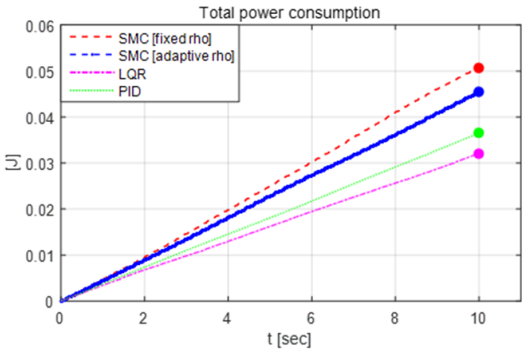

Fig. 21. Total power consumption: case 1-2.

Case 2-1: sinusoidal input without attachment

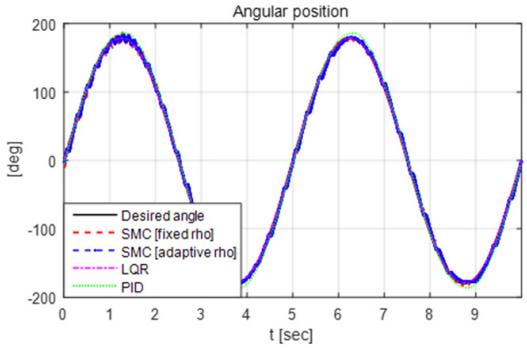

(a) Angles

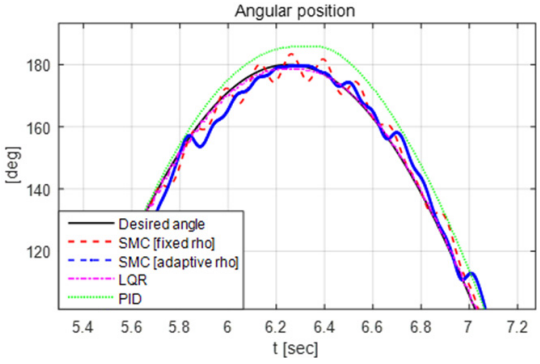

(b) Angles (zoom in)

Fig. 22. Desired and angular positions: case 2-1.

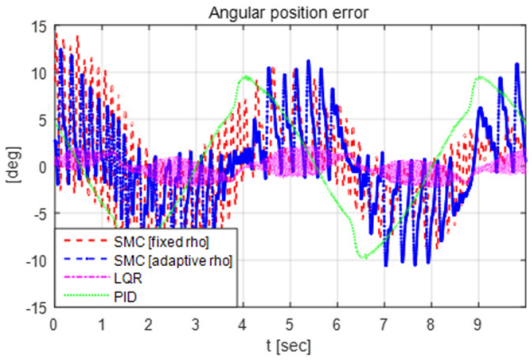

Fig. 23. Angular position errors: case 2-1.

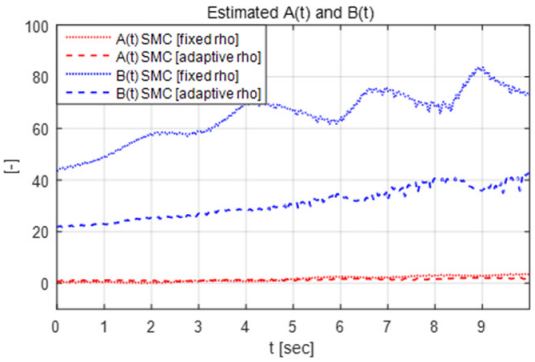

Fig. 24. Estimated parameters: case 2-1.

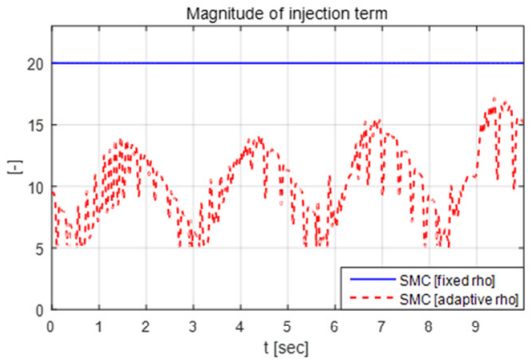

Fig. 25. Magnitude of injection term: case 2-1.

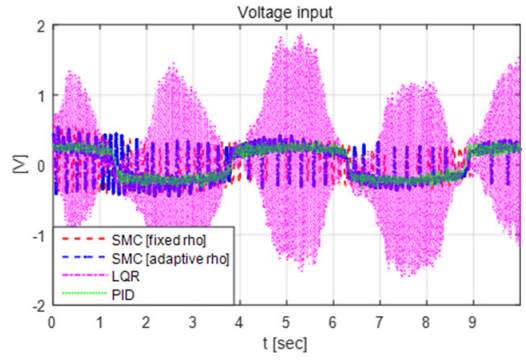

Fig. 26. Input voltage: case 2-1.

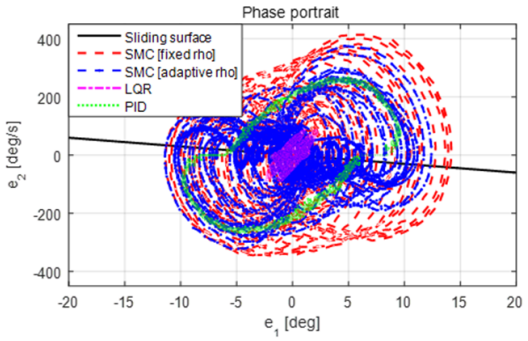

Fig. 27. Phase portrait: case 2-1.

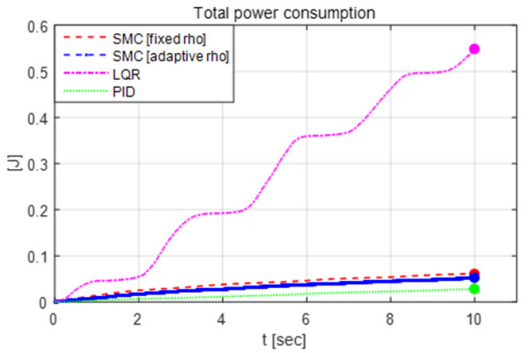

Fig. 28. Total power consumption: case 2-1.

Case 2-2: sinusoidal input with attachment

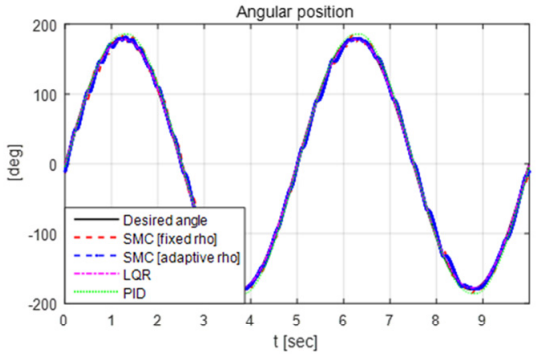

(a) Angles

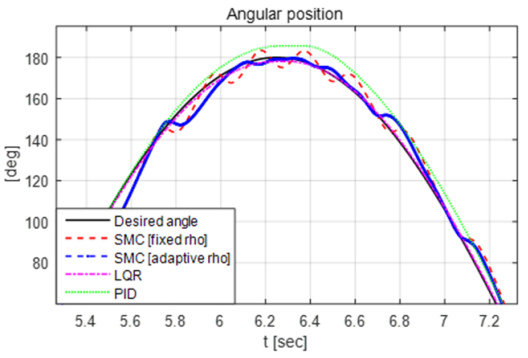

(b) Angles (zoom in)

Fig. 29. Desired and angular positions: case 2-2.

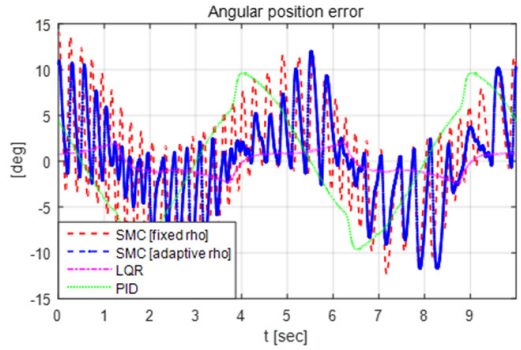

Fig. 30. Angular position errors: case 2-2.

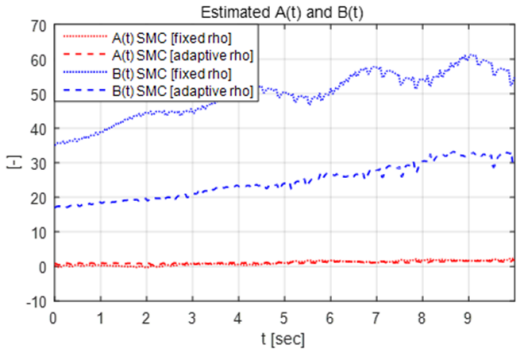

Fig. 31. Estimated parameters: case 2-2.

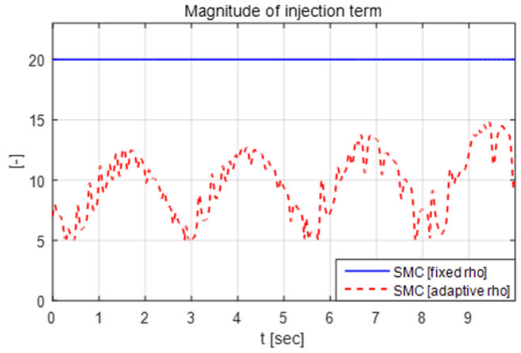

Fig. 32. Magnitude of injection term: case 2-2.

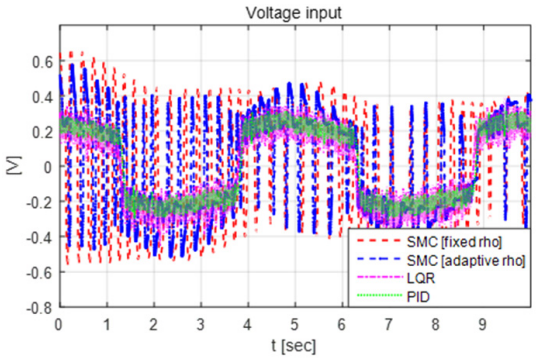

Fig. 33. Input voltage: case 2-2.

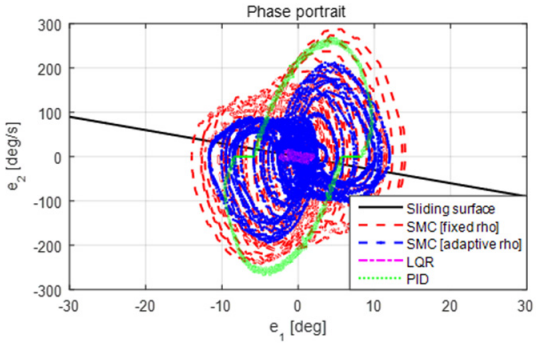

Fig. 34. Phase portrait: case 2-2.

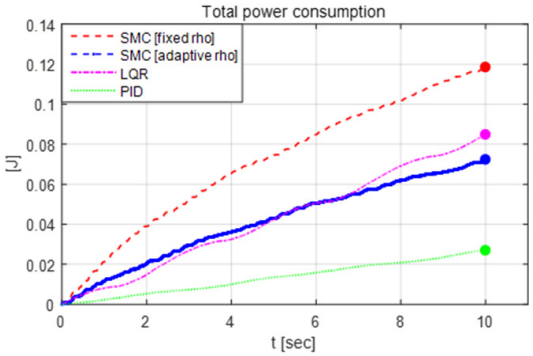

Fig. 35. Total power consumption: case 2-2.

The results of the motor angles, parameter estimation, magnitude of injection term, applied input voltage, phase portrait, and total power consumption were analyzed for the performance evaluation of the designed control algorithms. As shown in the control error graphs (Figs. 8, 9, 15, 16, 22, 23, 29 and 30), the PID and LQR controller show a relatively more accurate control compared to the two different SMC controllers in cases 1-1 and 1-2. However, the PID has limitations in that a pre-turning of the control gains is needed to guarantee good tracking capabilities, and the control performance can vary according to the parameter uncertainties (e.g., variations of the load conditions). As a major concern of the LQR, it requires accurate system parameters for mathematical modeling and computation of the optimal control inputs, and its control performance is subject to uncertainties.

The system parameters $A(t)$ and $B(t)$ were estimated for calculations of the control input (input voltage) using Eq. (27). As seen in Figs. 10, 17, 24 and 31, the estimated system parameters in each case have different values in real-time. However, the designed SMC with a self-tuning rule can trace the desired input reasonably. An analysis of tracking control errors is as follows. It is observed that there is a relatively large variation of the error values between cases 1-1 and 2-1 (Figs. 9 and 23) and cases 1-2 and 2-2 (Figs. 16 and 30) for the SMC (with fixed rho), LQR, and PID controllers when the type of desired input is changed. However, there are no large variations in the error values between cases 1-1 and 2-1 (SMC with adaptive rho) and cases 1-2 and 2-2 (SMC with adaptive rho) in com-

Table 7. Error analysis.

Cases	Controller type	Error [RMS]
Case 1-1	SMC [fixed rho]	1.1168 deg
	SMC [adaptive rho]	2.0072 deg
	LQR	1.3634 deg
	PID	0.1017 deg
Case 1-2	SMC [fixed rho]	1.5971 deg
	SMC [adaptive rho]	2.1055 deg
	LQR	1.7447 deg
	PID	0.0654 deg
Case 2-1	SMC [fixed rho]	4.7545 deg
	SMC [adaptive rho]	4.7083 deg
	LQR	1.0206 deg
	PID	5.9455 deg
Case 2-2	SMC [fixed rho]	5.9313 deg
	SMC [adaptive rho]	4.7805 deg
	LQR	1.2131 deg
	PID	5.9534 deg

Table 8. Power consumption analysis.

Cases	Controller type	Power consumption
Case 1-1	SMC [fixed rho]	0.0303 J
	SMC [adaptive rho]	0.0271 J
	LQR	0.0294 J
	PID	0.0352 J
Case 1-2	SMC [fixed rho]	0.0507 J
	SMC [adaptive rho]	0.0455 J
	LQR	0.0321 J
	PID	0.0365 J
Case 2-1	SMC [fixed rho]	0.0613 J
	SMC [adaptive rho]	0.0520 J
	LQR	0.5483 J
	PID	0.0280 J
Case 2-2	SMC [fixed rho]	0.1185 J
	SMC [adaptive rho]	0.0724 J
	LQR	0.0848 J
	PID	0.0271 J

parison with the SMC (with a fixed rho), LQR, and PID controllers. In the phase portraits shown in Figs. 13, 20, 27 and 34, it is observed that the SMC occupies a relatively larger region in the phase plane than the regions occupied by the LQR and PID controllers. However, the SMC system can be still considered stable because its error states are within the limited regions. The results of the magnitude of injection term (Figs. 11, 18, 25 and 32) and input voltage (Figs. 12, 19, 26 and 33) show that the SMC with self-tuning rule uses a smaller injection term than one with fixed injection term. This implies that an unnecessary input can be removed through a self-tuning rule, and therefore the energy efficiency can be improved. Table 7 shows the summarized RMS error values for each evaluation case. In cases 1-1 and 1-2, the RMS error values of the SMC with an adaptive rho are slightly larger than the error values of the SMC with a fixed rho. However, the RMS error values are within approximately 2 deg (ramp input) and 5 deg (sinusoidal input) for all four cases.

Table 8 summarizes the power consumption for each evaluation case. It was observed that the power consumption of all SMC, LQR, and PID controllers increases after a load is attached when the sinusoidal reference input is used (Figs. 28 and 35). Because the controller should consume more energy to change the direction of the motor with a relatively large rotational inertia, more energy is consumed to overcome the inertia. Similar results can be found in case of using a ramp input for all controllers except the PID in which the power consumption is slightly decreased after a load is attached (Figs. 28 and 35).

In addition, the power consumption of the SMC with an adaptive rho that adopts the proposed self-tuning rule is smaller than the SMC with a fixed rho of approximately 18.72 % on average for all cases (Figs. 14, 21, 28 and 35), while maintaining reasonable control errors (approximately 2 deg in case 1, and 5 deg in case 2).

The results in the figures and tables clearly show that the SMC algorithm with a self-tuning rule can achieve versatility with tracking accuracy and energy saving without knowing any system parameters in comparison with that of conventional LQR, PID, and SMC controllers with a fixed injection term. The performance of the control algorithm (SMC with adaptive rho) proposed in this study is summarized as follows.

A. Case 1-1 (ramp input, w/o load)
: Error → RMS error within approximately 2 deg
: Power consumption → the lowest power consumption
B. Case 1-2 (ramp, w/ load)
: Error → RMS error within approximately 2 deg
: Power consumption → smaller than SMC with a fixed rho
C. Case 2-1 (sinusoidal input, w/o load)
: Error → RMS error within approximately 5 deg
: Power consumption → smaller than SMC with a fixed rho
D. Case 2-2 (sinusoidal, w/ load)
: Error → RMS error within approximately 5 deg
: Power consumption → smaller than SMC with a fixed rho

Based on the control algorithm of the SMC with RLS estimation and a self-tuning rule, the desired angular position can be tracked efficiently without the use of any system parameters.

5. Conclusion

This paper proposed a self-tuning rule-based adaptive sliding mode control algorithm for DC motor position control using the RLS method. To control the angular position of the DC motor, the system parameters were estimated using RLS with multiple forgetting factors. Based on the estimated parameters, the sliding mode control algorithm was designed and its stability verified mathematically using Eqs. (23)-(27). The magnitude of

the injection term in the sliding mode control algorithm was tuned using a self-tuning rule. The main contributions of this study can be summarized as follows.

First, the angular position of the DC motor can be controlled robustly despite load variations and parameter uncertainties because the parameters including the load can be estimated through RLS in real-time. In other words, the proposed position control algorithm does not require any system parameters. Second, energy efficiency can be improved because the unnecessary input is removed through the self-tuning rule. The performance of the control algorithm was compared with conventional controllers such as PID and LQR controllers. The evaluation results indicate that compared to the conventional control algorithms, the designed SMC algorithm with a self-tuning rule can provide an effective control solution that can deal with both tracking accuracy and energy efficiency without prior knowledge of the system. However, there are certain limitations to the parameter estimation and self-tuning rule described herein. For the parameter estimation, it was not verified whether the estimated parameters can represent the actual dynamics of a system in real-time. In addition, the minimum value and increasing ratio applied in the self-tuning rule were determined empirically. Furthermore, the designed control algorithm can be improved through future work by considering constraints of an input limit or by integrating it with the model predictive control technique to predict the system's dynamic behavior. Finally, it is expected that the proposed adaptive control algorithm can be used for various industries that require an angular position control and extended to the study on fault diagnosis and tolerant control of DC motors.

Nomenclature

v_m : Input voltage of a DC motor
R_m : Resistance of a DC motor
i_m : Current of a DC motor
L_m : Inductance of a DC motor
ω_m : Angular velocity of a DC motor
J : Rotational inertia of a DC motor
τ_m : Motor torque
θ : Estimate of recursive least squares
ϕ : Regressor of recursive least squares
v : Injection term of sliding mode controller
ρ : Magnitude of Injection term

References

[1] D. T. Liem, D. Q. Truong and K. K. Ahn, A torque estimator using online tuning grey fuzzy PID for applications to torque-sensorless control of DC motors, *Mechatronics*, 26 (2015) 45-63.

[2] L. F. Jesus, J. Reger and H. S. Ramirez, Load torque estimation and passivity-based control of a boost-converter/DC-motor combination, *IEEE Transactions on Control System Technology*, 18 (6) (2010) 1398-1405.

[3] D. Shah, R. Ortega and A. Astolfi, Speed and load torque observer for rotating machines, *Proceedings of the 48th IEEE Conference on Decision and Control (CDC) held jointly with 2009 28th Chinese Control Conference* (2009) 6143-6148.

[4] T. Shi, Y. Cao, G. Jiang, X. Li and C. Xia, A torque control strategy for torque ripple reduction of brushless DC motor with nonideal back electromotive force, *IEEE Trans. Ind. Electron*, 64 (6) (2017) 4423-4433.

[5] A. Rubaai and P. Young, Hardware/software implementation of fuzzy-neural-network self-learning control methods for brushless DC motor drives, *IEEE Trans. Ind. Appl*, 52 (1) (2015) 414-424.

[6] Y. Hu, W. Gu, H. Zhang and H. Chen, Adaptive robust triple-step control for compensating cogging torque and model uncertainty in a DC motor, *IEEE Transactions on Systems, Man, and Cybernetics: Systems* (2018) 1-10.

[7] N. D. Dao and D. C. Lee, Operation and control scheme of a five-level hybrid inverter for medium-voltage motor drives, *IEEE Trans. Power Electron*, 33 (12) (2018) 10178-10187.

[8] S. You, J. Gil and W. Kim, Extended state observer based robust position tracking control for DC motor with external disturbance and system uncertainties, *J. Electr. Eng. Technol.*, 14 (4) (2019) 1367-1646.

[9] A. Rodríguez-Molina, M. G. Villarreal-Cervantes and M. Aldape-Pérez, An adaptive control study for the DC motor using meta-heuristic algorithms, *Soft Computing*, 23 (3) (2019) 889-906.

[10] P. Kofinas and A. Dounis, Fuzzy Q-learning agent for online tuning of PID controller for DC motor speed control, *Algorithms*, 11 (10) (2018) 1-13.

[11] K. Premkumar and B. V. Manikandan, Bat algorithm optimized fuzzy PD based speed controller for brushless direct current motor, *Engineering Science and Technology, An International Journal*, 19 (2) (2016) 818-840.

[12] K. Premkumar and B. V. Manikandan, Speed control of brushless DC motor using bat algorithm optimized adaptive neuro-fuzzy inference system, *Appl. Soft Comput*, 32 (2015) 403-419.

[13] G. G. Rigatos, Adaptive fuzzy control of DC motors using state and output feedback, *Electr. Power Syst. Res*, 79 (11) (2009) 1579-1592.

[14] P. S. Londhe, B. M. Patre and A. P. Tiwari, Fuzzy-like PD controller for spatial control of advanced heavy water reactor, *Nucl. Eng. Des,* 274 (2014) 77-89.

[15] S. Sharma, K. P. S. Rana and V. Kumar, Performance analysis of fractional order fuzzy PID controller applied to a robotic manipulator, *Expert Syst. Appl*, 41 (9) (2014) 4274-4289.

[16] T. A. Zarma, B. M. Mustapha, H. U. Suleiman, A. A. Galadima, E. C. Ashigweke and S. Thomas, Torque control in brushless DC motor using intelligent linear quadratic regulator controller, *IEEE 7th International Conference on Adaptive Science and Technology* (2018) 1-7.

[17] C. F. Hsu and B. K. Lee, FPGA-based adaptive PID control of a DC motor driver via sliding-mode approach, *Expert Syst. Appl*, 38 (9) (2011) 11866-11872.

[18] S. Mondal and C. Mahanta, Adaptive second order terminal sliding mode controller for robotic manipulators, *Journal of the Franklin Institute*, 351 (2013) 2356-2377.
[19] V. Utkin and A. Poznyak, Adaptive sliding mode control with application to super-twist algorithm: equivalent control method, *Automatica*, 49 (1) (2013) 39-47.
[20] A. K. Mollaee and H. Tirandaz, Estimation of load torque in induction motors via dynamic sliding mode control and new nonlinear state observer, *Journal of Mechanical Science and Technology*, 32 (5) (2018) 2283-2288.
[21] A. Vahidi, A. Stefanopoulou and H. Peng, Recursive least squares with forgetting for online estimation of vehicle mass and road grade: theory and experiments, *Veh. Syst. Dyn*, 43 (1) (2005) 31-55.
[22] Y. Shtessel, C. Edwards, L. Fridman and A. Levant, *Sliding Mode Control and Observation*, 1st Ed., Springer, New York (2010) 43-99.
[23] Y. T. Oh and S. I. Han, Finite-time sliding mode joint positioning error constraint control for robot manipulator in the presence of unknown deadzone, *Journal of Mechanical Science and Technology*, 32 (2) (2018) 875-884.

Kwangseok Oh received a B.S. degree in Mechanical Engineering from Hanyang University, Seoul in 2009 and an M.S. degree and a Ph.D. in Mechanical and Aerospace Engineering from Seoul National University, Seoul in 2013 and 2016. From 2016 to 2017, he was an Assistant Professor in the Automotive Engineering Department at Honam University. Since 2017, he has been an Assistant Professor in the Mechanical Engineering Department of Hankyong National University, Anseong-Si, South Korea. His research interests include fail-safe systems for autonomous driving, adaptive and predictive control.

Jaho Seo received his B.S. degree in Agricultural Machinery and Process Engineering from Seoul National University, Seoul, Korea in 1999, his M.E. degree in Mechanical Engineering from University of Quebec (Ecole de Technologie Superieure), Montreal, Canada in 2006, and his Ph.D. in Mechanical Engineering from University of Waterloo, Waterloo, Canada in 2011. He was with the Department of Mechanical and Mechatronics Engineering of University of Waterloo as a postdoctoral fellow in 2011, the Department of System Reliability of Korea Institute of Machinery & Materials (KIMM) as a Senior Researcher during 2012-2016, and the Department of Biosystems Machinery Engineering of Chungnam National University, Korea as an Assistant Professor during 2016-2017. Since 2017, he has been an Assistant Professor at the Department of Automotive and Mechatronics Engineering, Ontario Tech University where he has been involved in research on the development of autonomous control systems for intelligent mobile machines.